IRSTI 31.19.15 https://doi.org/10.26577/IJBCh2024v17i1-a9

I.Yu. Silachyov[1*], V.A. Glagolev[2], M.N. Kokkuzova[2]

[1]Institute of Nuclear Physics, Almaty, Kazakhstan
[2]Institute of Geological Sciences named after K.I. Satpayev, Almaty, Kazakhstan
*e-mail: silachyov@inp.kz
(Received 17 May 2023; received in revised form 15 September 2023; accepted 3 November 2023)

Gold content determination in small core-samples by instrumental neutron activation analysis

Abstract. Application of instrumental neutron activation analysis (INAA) based on the relative method of concentration standardization was considered to determine Au content in small solid core-samples of the gold-bearing ores and rocks up to 10 g of the mass. The small core-samples about 10 mm in diameter and 22-23 mm in length were cut from the previously collected ore lumps or in-situ using a handheld drilling rig. The studied small core-samples and the polyethylene capsules of the same dimensions filled up with the corresponding certified reference material (CRM) were irradiated for 2 min by a lower density neutron flux with the help of the automated pneumatic transport system (PTS). Maximum mass and dimensions of the core-samples corresponded to the PTS design and to the conditions of its safe operation. A special device was made to fix the transport capsules in the stable counting geometry making possible to eliminate the influence of the neutron flux gradient during irradiation. Due to the substantial differences in CRM and solid sample densities, corrections for neutron self-shielding and for gamma-ray self-absorption by the core-samples were applied. The method was tried to analyze Au content in 170 small core-samples presenting different gold-bearing ores and country rocks from the Kazakhstan's gold-barite-polymetallic deposit Maikain. This approach, rather simple methodically and requiring no unique equipment, can be used to assess gold resources together with the methods of geostatistics.
Key words: Neutron activation analysis, gold, small core-samples.

Introduction

A main problem of gold dependable determination in ores and gold-bearing rocks comes from its extremely heterogeneous distribution. Together with finely dispersed "invisible" forms such as colloidal, cluster, and chemically bound, gold occurs as dissemination in a range of minerals (pyrite, chalcopyrite, arsenopyrite, quartz, etc.) forming native grains or discrete particles highly variable in size [1-3]. Anomalously high gold contents may be also caused by the secondary enrichment processes. To improve reliability of gold analysis representative samples should be used including "multiple smaller aliquots of the same sample" or larger sample aliquots [4]. The size of the latter depends on the variety of factors and, hence, is discussible, but its mass is unanimously considered beginning from 10 g, leastwise [5]. This is a rather large amount which can be scarcely introduced if the most commonly spread destructive pretreatment is applied followed by a high-sensitive instrumental analytical technique. Moreover, the other challenges can arouse substantially diminishing reliability of gold content determination.

Firstly, grinding of geological samples presents a problem itself. Soft gold grains are resistant to milling and may be lost in one sample and contaminate the others via the milling vessels [6]. To avoid contamination, rock samples should be passed through the mill in the order of increasing of their gold content that is hardly possible before analysis.

On the other hand, Au mass fractions are frequently underestimated in silicates and in the resistant sulphide matrix due to incomplete dissolution when the classical acid digestion is applied, e.g. by aqua regia [7]. The popular up-to-date technique such as microwave-assisted pressure digestion at elevated temperatures is more effective and efficient, but all the same doesn't always solve the problem of complete sample decomposition. Its other disadvantages include a limited aliquot mass, complicated vessel constructions, and expensive equipment [8].

All these difficulties are avoided if the nondestructive pretreatment oriented to instrumental analytical techniques dealing with the intact larger samples can be applied. Advantages and limitations of such methods as laser ablation inductively coupled plasma mass spectrometry and high-energy instrumental photon activation analysis (IPAA) using both the reactions of isomeric state photoexcitation ^{197}Au(γ, γ)^{197m}Au and photoneutron production ^{197}Au(γ, n)^{196}Au, are discussed in [6] in the context of geochemical explorations. The last variant of IPAA is likely quite appropriate to analyze routinely large, up to 0.5 kg, rock samples for industrially significant gold mass fractions, except for the facilities to produce high-energy (20–30 MeV) gamma radiation – linear electron accelerators [9] or cyclotrons [10] – are mainly unique research installations.

Compact neutron generators to conduct the fast neutron (14 MeV) instrumental neutron activation analysis (INAA) are far more accessible [11, 12]. However, the sensitivity of gold determination is often insufficient due to a significantly (several orders of magnitude) lower flux density of 14 MeV neutrons comparing with the thermal neutron flux density σ_0 produced by nuclear reactors, as well as due to the low cross-sections of activation by the fast neutrons (≈2.1 barn,^{197}Au(n, 2n)^{196}Au and ≈1.6 barn,^{197}Au(n, 2n)^{196m}Au).

Comparing with the methods above, high-sensitive thermal neutron INAA (σ_0 = 98.7 barn, ^{197}Au(n, γ)^{198}Au), taking account of its advantages [5, 13, 14], seems being the most suitable method to analyze solid volumetric samples for Au content provided neutron self-shielding and gamma-ray self-absorption by the samples are considered, and the corrections for sample size deviation from the "point source" during irradiation and counting are made[15]. Different approaches both semi-empirical and theoretical are developed to evaluate and account these corrections mainly for the regular-shaped (cylindrical) samples [16, 17]. If the internal standard method (ISM) is used in comparator INAA, the corrections are basically reduced to zero or minimized. Moreover, irregular-shaped samples can be analyzed in this case too [18].

The ISM based comparator INAA was tried in the previous investigation [6] to determine Au content in the puck-like common rock samples 15–20 g of the mass which were cut off from the corresponding drill-cores. Fe mass fraction in the same volumetric samples by X-ray fluorescence (XRF) method was used as the internal standard. Only homogenous rocks with respect to the internal comparator content can be reliably analyzed using this approach. Therefore, it is restricted by geochemical explorations of some types of more or less homogenous magmatic and metamorphic rocks characterized by Au contents close to that of the upper continental crust (UCC).

Subsequent investigations showed a great scope of heterogeneity for the similar puck-like samples cut off from the gold-bearing rocks and ores such as quartzites, black shales, and polymetallic ores. None of the potential comparator elements (Fe, As, Rb, Ba) can be used as the internal standard due to substantial unreliability of their determination by XRF resulted from high heterogeneity of these elements' distribution both in the volume and on the surface of the samples. After irradiation and counting, the samples could be powdered to analyze them reliably for, e.g., Fe content, but this idea was abandoned for the reasons of radiation safety.

That is why another approach was tried in the present work consisting in implementing INAA of the small core-samples using the simple way of relative standardization. This became possible due to the advantages of irradiation in a distant channel out of the reactor active zone, as well as due to small sizes and regular cylinder shape of the core-samples, resulted in minimum of the corrections which should be accounted. The method was applied to determine Au content both in the ores and some country rocks of the mined Maikain deposit in Kazakhstan.

Materials and methods

Gold-barite-polymetallic deposit Maikain is located in Bayanaul district of the Pavlodar region, North-Eastern Kazakhstan. The gold-bearing ores form several associations differing in Au content. Gold occurs as inclusions in all main ore minerals, quartz and barite displaying irregular mottling. Native gold is found as intergrowth with bornite forming thin veins. The sizes of gold particles are 20 to 50 μm, sometimes up to 200 μm [19, 20].

A part of the studied geological material – lumps of ores and country rocks – was collected by M.Kokkuzova and delivered to a Satpayev Institute's laboratory. Several small core-samples were drilled out from every lump using a piped core bit with diamond chisels (inner diameter is 10 mm) installed into a portable drill. Then the billets were cut with a diamond saw to get the right cylinders 22-23 mm in length. The lump remainders were crashed and ground to the particle size about 0.07 mm to investigate them as the combined powder samples corresponding to several core-samples of the same origin.

Sizes of the small core-sample were selected to fit the dimensions of the standard HDPE capsules (inserted in the transport ones) to implement relative method of standardization. The masses of core-samples were evaluated preliminarilyy; none of them should exceed ≈10 g to provide safe operation of the automated pneumatic transport system (PTS) [21, 22], i.e. to avoid capsule jamming during irradiation.

The other samples under investigation were taken by V. Glagolev *in situ*, using the same equipment, from the different areas of Maikain deposit including the opencast workings and one or two new cites cleared from the surface to revise ore resources. The small core-samples of different geological objects were drilled out as close as possible one to another. Lumps of the same rocks were collected too to prepare powdered samples.

All cylinder samples turned out practically identical, even enough and without visible faults. Exterior view of several small core-samples drilled out of the same geological object is shown on Figure 1. As much as 170 volumetric samples were prepared on the whole.

Figure 1 – Three small core-samples drilled out from the lump sample M2322 (banded quartz ore)

Masses of the core-samples were determined up to the third decimal with a Mettler Toledo analytical balance. Diameter of the cylinder samples depending on the piped core bit was ascribed to 9.5 ± 0.2 mm; the height was measured with a caliper within the accuracy ± 0.5 mm. Based on these data, the combined relative standard uncertainty (δ_ρ) of the sample density evaluation was assessed [23] (δ_ρ is used below to evaluate expanded uncertainty of Au determination) – about 3.5%.

Unlike the objects which were being studied earlier during geochemical explorations [6] the mined Maikain deposit is characterized by much more Au contents. Hence short irradiation time and/or lower density of the thermal neutron flux Φ_{th} are enough to implement INAA. Therefore, the horizontal channel of the WWR-K research reactor (INP, Almaty) equipped with PTS was selected. Φ_{th} value in this channel is approximately one twentieths comparing with that (≈ 9×10^{13} cm^{-2} s^{-1}) in the vertical channel used to irradiate the samples [24, 25]. Since the PTS terminal is isolated from the reactor active zone cooled by water, there wasn't need to seal the samples in polyethylene before irradiation. The other advantages of the horizontal channel include invariability of the irradiation geometry and hence the same neutron flux gradient for the equal length cylinder samples, simple operation, promptness, and independence of the reactor personal. The limited mass of the studied samples comparing with irradiation in the vertical channels is a certain disadvantage, but the used PTS wasn't initially designed to transport heavy objects.

To conduct INAA, the small core-samples were fixed in the center of the HDPE transport capsules and irradiated one by one for 2 minutes. This irradiation time was selected before to avoid overheating of the capsules inside the non-cooled PTS terminal.

The corresponding powder samples intended for the detailed geochemical investigations were prepared for irradiation in the vertical channel No.10-6 of WWR-K in the usual manner [25]. Approximately 100 mg of the assays were sealed in plane double polyethylene bags and packed batchwise in aluminium foil. Every batch included a dozen samples and a neutron flux monitor (≈10 mg of ZrO_2, the Institute of Reference Materials, Ekaterinburg, Russian Federation). No samples of certified reference material (CRM) were involved since the comparator model of concentration standardization based on the internal standard method was conceived [6, 21, 24]. All the packages were independently irradiated for 2.5 h.

Gamma-spectrometric measurements of the small core-samples were carried out for 20 minutes 7 days later when radionuclide ^{76}As substantially decayed. The following equipment was used: a coaxial HPGe detector GC2018 with a horizontal dipstick cryostat (Canberra, 20% of a relative efficiency, and 1.80 keV at the 1332 keV peak of ^{60}Co of an energy resolution) and a Canberra multi-channel analyzer DSA-1000, both incorporated into PTS.

Counting geometry was organized in a manner making possible to eliminate the influence of the neutron flux gradient in the irradiation terminal directed along the transport capsule axis. The special

Plexiglas attachment was made and mounted on the detector cap to fix the transport capsules parallel to the cap's plane surface as Figure 2 demonstrates. The small core-samples are located in the same position 25 mm distant from the detector cup, right opposite to its centre. That is the way the central symmetry of the counting geometry was achieved.

Figure 2 – HPGe detector GC2018 with the Plexiglas attachment on its cap and a HDPE transport capsule held by a tweezers

The powder samples were counted for Au (and some other element) content for 40 minutes after 12–14 days of decay using an extended-range HPGe detector GX5019 (Canberra, 50% of a relative efficiency, and 1.86 keV of an energy resolution) and the similar multi-channel analyzer. All the samples were placed at the distance of 24 mm from the detector cap.

Both detectors were calibrated for relative detection efficiency with the help of a multi-gamma ray standard MGS-1 (^{152}Eu, ^{154}Eu, ^{155}Eu) also by Canberra.

GENIE 2000 software was used for spectra collection in the first case, and the "AnalGamma" software developed in the INP – to analyze the powder samples. The last one was applied for spectra treatment as well, in the same way as before, e.g. [25].

Practically, there are no unresolved spectral interferences to the intensive analytical gamma-line of the radionuclide ^{198}Au (411.80 keV of the energy E) which should be accounted, especially when gold ore samples are analyzed. Only in the case of country rock investigation count rate of ^{198}Au was corrected by that of the low-intensive gamma-line of ^{152}Eu (E = 411.12 keV).

Fe content of the powder samples used as the internal standard to determine their Au mass fraction by comparator INAA was determined by XRF technique with a portable energy dispersive X-ray spectrometer RLP-21T by JSC "AspapGeo" (Almaty, Kazakhstan). This spectrometer is applied constantly to support comparator INAA and was mentioned in the previous investigations more than once. RLP-21T is enrolled in the State Register of Measuring Devices (Certificate № 670, valid to 27.07.2025), and the corresponding analytical technique is registered by the National Body for Certification of Kazakhstan (Certificate No. 69-2022, valid till 15.02.2027).

Results and discussion

Gold content C_a (ppm) of the analyzed small core-samples was calculated as follows according to a variant of the relative method of concentration standardization:

$$C_a = \frac{J_a D_a}{G_a F_a m_a t_{irr}^a K_r}, \quad (1)$$

where J_a is net peak count rate of ^{198}Au analytical gamma-line (cps); $D_a = \exp(-\lambda_{Au}(7 - t_d)$ is decay factor depending on ^{198}Au decay constant λ_{Au} and decay time t_d after the end of irradiation (D_a is normalized to t_d = 7 d for convenience); G_a is the correction factor for neutron self-shielding by the samples; F_a is the correction factor for the analytical gamma-ray self-absorption by the sample; m_a is the sample mass (g); t_{irr}^a is irradiation time (min).

Coefficient K_r (cps ppm^{-1} g^{-1} min^{-1}) can be determined by the similar way with the help of a number of CRMs certified for Au content:

$$K_r = \frac{J_r D_r}{G_r F_r C_r m_r t_{irr}^r}. \quad (2)$$

K_r corresponds to ^{198}Au analytical gamma-line count rate J_r after 7 d of decay (corrected by the factors G_r and F_r) per m_r = 1 g of a CRM with gold content C_r = 1 ppm irradiated for t_{irr}^r = 1 min. Under the conditions of a stable neutron flux density in the irradiation channel equipped with PTS, for the same sample dimensions, irradiation and counting geometries, K_r is practically invariable.

To evaluate K_r the next four CRMs were selected: OSO 163 and OSO 165 by the All-Russian Scientific-Research Institution of Mineral Resources (Moscow), GSO 1789 by the Vinogradov Institute of Geochemistry (Irkutsk, Russian Federation), and OREAS 684 by Ore Research & Exploration (Australia). Four standard HDPE capsules close by their inner dimensions to the analyzed core-samples (22 mm of the height and 10 mm across the diameter) were filled up tightly with these CRMs and then welded all around. Since more than 2 g of the matter were tampered into the capsules (Table 1), the assays can be considered representative enough, despite the CRMs were produced from natural gold-bearing ores. Moreover, homogeneity of the CRMs was confirmed by their previous utilization in INAA.

Table 1 – Au content of four small volumetric CRM samples (P = 0.95), their masses, densities and correction factors for self-absorption of the 411.8 keV gamma-ray

CRM name	CRM type	m_r, g	ρ_r, g cm^{-3}	F_r	Au, μg g^{-1} (ppm)	
					Certified value	Measured value
OSO 163	Gold-bearing ore	2.286	1.386	0.945	0.91 ± 0.02	0.889 ± 0.075
OSO 165	Gold-bearing ore	2.223	1.348	0.947	6.0 ± 0.1	6.08 ± 0.48
GSO 1789	Gold-bearing ore	2.180	1.322	0.948	4.5 ± 0.1	4.61 ± 0.39
OREAS 684	Platinum group element ore	2.239	1.358	0.946	0.248 ± 0.007	0.244 ± 0.022

The capsules were irradiated for 1-3 min depending on Au content and counted in the same way as the investigated core-samples.

Correction factor for the neutron self-shielding G_r for Au was assessed with the help of the spreadsheet by C. Chilian et al. [26] supposing that major element contents in the samples correspond to that of UCC [27], and Sm, Eu and Gd mass fractions characterized by the maximum values of the thermal neutron cross-section are equal to their UCC values [28]. With the CRM masses presented in Table 1 the factor G_r is close to unity (0.991) and doesn't depend on Au content up to 100–200 μg g^{-1}.

Correction factor for the ^{198}Au analytical gamma-ray self-absorption F_r was evaluated following the next expression:

$$F_r = \frac{1-\exp(-\rho_r \mu_\Sigma(E_{\mathrm{Au}})h_r}{\rho_r \mu_\Sigma(E_{\mathrm{Au}})h_r}, \qquad (3)$$

where ρ_r is core-sample density (g cm^{-3}); $\mu_\Sigma(E_{\mathrm{Au}})$ – total photon mass coefficient of ^{198}Au analytical gamma-line attenuation (cm^2 g^{-1}); and h_r – effective sample thickness (cm). Equating the area of the cylinder sample base to the equal-area square, h_r was taken equal to 0.886 cm. Individual $\mu(E_{\mathrm{Au}})$ values for the main rock-forming oxides were picked up from a NIST database [29]. These values are very close one to another since interaction of the high-energy gamma-rays with the matter is mainly brought to the scattering processes. The issue is discussed in [6] in more details. $\mu_\Sigma(E_{\mathrm{Au}})$ = 0.0927 cm^2 g^{-1} corresponding to the composition of UCC is accepted to assess F_r. The values of F_r factor for four CRMs are presented in Table 1. F_r values depend linearly on the sample density up to 5 g cm^{-3}, i.e. including heavy rocks, therefore relative uncertainty of F_r factor evaluation can be accepted equal to δ_ρ (see above).

Thus, taking account of the considerations above, four assessments of K_r coefficient were made according to Eq. 2. The mean value K_r = 0.9686 was used to calculate Au content in the small core-samples (Eq. 1), and its relative standard deviation δ_{Kr} = 2.2 % – to evaluate uncertainty of the results.

Expanded uncertainty of Au determination $U(C_a)$ was estimated as follows (P = 0.95):

$$U(C_a) \approx 2C_a\sqrt{\frac{u(J_a)^2}{J_a^{\,2}} + (\delta_\rho)^2 + (\delta_K)^2}, \qquad (4)$$

where $u(J_a)$ is the standard uncertainty of J_a, δ_ρ and δ_{Kr} are evaluated above (all the summands are in %). Relative uncertainties of m and t^a_{irr} measuring (Eq. 1) are far lower than the terms accounted by Eq. 4 and are hence ignored. G_a is considered a constant.

The results of four small volumetric CRM analysis for Au content using Eq. 1 (P = 0.95) are presented in Table 1. The measured values differ from the certified ones by no more than 2.5%. Expanded uncertainty

doesn't exceed the allowable standard deviation of the results of Au determination according to the III category of precision (of analysis) (12-30% for the intervals including these contents) according to OST 41-08-221-04 [30], for samples with fine-dispersed gold particles <0.1 mm of the size].

Unlike few CRMs above which were irradiated practically simultaneously, 16 days were spent to irradiate all the studied small core-samples divided into a range of parties. To take account of possible K_r diminishing for such a long time due to nuclear fuel burn-out in the WWR-K active zone (the reactor is halted every three weeks to replace a part of uranium fuel elements), one more set of the same CRMs was prepared and irradiated in the end of the investigation. The assessed K_r value decreased by 5% only, so linear interpolation with time of the coefficient was used to calculate Au contents (Eq. 1).

Table 2 – Gold content in the small core-samples and corresponding powder samples collected from the gold-polymetallic deposit Maikain, ore material (P = 0.95)

Sample number	Description	Core-sample			Powder sample
		Mass, g	Density, g cm^{-3}	Au, μg g^{-1} (ppm)	
M1859	Pyrite-barite-polymetallic ore	6.854 6.826 6.944 7.385 6.545	4.21 4.19 4.36 4.34 4.02	1.27 ± 0.11 1.26 ± 0.11 1.67 ± 0.14 1.56 ± 0.13 1.23 ± 0.11	1.30 ± 0.13
M2124	Pyrite-barite-polymetallic ore	7.354 7.509 7.275 7.678 7.299	4.51 4.51 4.47 4.52 4.48	2.09 ± 0.18 2.47 ± 0.21 1.23 ± 0.11 1.30 ± 0.11 1.54 ± 0.13	1.64 ± 0.16
M1998	Copper-pyrite ore	7.571 7.558 7.893 7.519 7.346	4.45 4.54 4.55 4.52 4.51	8.31 ± 0.71 10.0 ± 0.8 5.54 ± 0.47 9.18 ± 0.78 7.47 ± 0.63	6.41 ± 0.61
M2052	Copper-pyrite ore	7.290 7.381 7.309 7.098 7.462	4.47 4.53 4.49 4.36 4.39	2.79 ± 0.24 5.09 ± 0.43 9.19 ± 0.77 5.45 ± 0.46 1.90 ± 0.16	2.80 ± 0.26
M2514	Sulphide ore	7.678 7.539 7.043 7.570 7.685	4.61 4.73 4.52 4.65 4.72	0.292 ± 0.026 0.251 ± 0.023 0.311 ± 0.028 0.251 ± 0.023 0.277 ± 0.025	0.342 ± 0.034
M2684	Sulphide-polymetallic ore	6.911 6.601 6.757 6.505 6.836	4.15 4.14 4.06 3.99 4.11	2.63 ± 0.22 2.75 ± 0.23 2.44 ± 0.21 2.62 ± 0.22 2.71 ± 0.23	2.49 ± 0.24
M2691	Quartz sulphide ore	4.983 4.790 4.621 5.118 4.879	2.99 2.88 2.78 2.95 2.81	1.61 ± 0.14 3.20 ± 0.27 2.66 ± 0.23 0.906 ± 0.077 1.67 ± 0.14	1.51 ± 0.14

Table continuation

Sample number	Description	Core-sample			Powder sample
		Mass, g	Density, g cm^{-3}	Au, μg g^{-1} (ppm)	
M2821	Quartz sulphide ore	6.921	4.16	0.525 ± 0.047	0.647 ± 0.063
		6.767	4.15	1.21 ± 0.10	
		7.032	4.22	0.333 ± 0.030	
		7.180	4.31	0.376 ± 0.034	
		7.144	4.29	0.461 ± 0.040	
M2322	Banded quartz ore	5.336	3.28	0.684 ± 0.059	1.19 ± 0.11
		4.500	2.70	0.365 ± 0.033	
		4.539	2.79	0.560 ± 0.049	
		4.917	3.09	0.575 ± 0.050	
		5.264	3.16	0.312 ± 0.028	

The other distinction between powder CRM and core-sample investigation consists in the substantially higher density of the latter reaching approximately 2.5–4.5 g cm^{-3} depending on the rock type. It results in small diminishing of G_a factor value to no less than 0.970 for the densest samples using the spreadsheet above. F_a factor varies in the broader range about 0.91–0.84 for the same interval of core-sample density.

At last, taking account of the high ratio of the resonance integral to the thermal neutron cross-section the isotope ^{197}Au is characterized (15.7 [31]), invariability of thermal to epithermal neutron flux ratio f in the beginning and in the end of core-sample irradiation was verified. The mentioned ZrO_2 flux monitors were used with this end in view, enlarged to ≈100 mg to compensate the lower neutron flux ratio in the horizontal channel. Two f values estimated using the "bare bi-isotopic method", e.g. [25], actually did not differ from one another being close to the mean value 85.0 ± 3.5 assessed for the long observation period.

As an example, the results of Au content determination in several samples (as they were documented) presenting different types of the Maikain's gold-bearing ores are demonstrated in Table 2. Five small core-samples were cut off from each sample, and the corresponding values of their mass and density are added to the table too. The last column shows the results of Au determination in the powder samples prepared as mentioned above.

Almost all ores displayed low density variations, no more than 8%, due to their composition variability, except for the banded quartz ore (up to 18%). Unlike this, gold revealed high degree of heterogeneity within the samples, especially for quartz and some polymetallic ores: Au contents in the small core-samples cut off from one lump differ three-five times. Sulphide ores turned out far more homogeneous in this respect.

The average gold mass fractions in the core-samples differ from that of the powdered samples to various extents, up to more than twice, and there may be a range of reasons for it. In any case, these powder samples, as they were prepared, seem far from being representative. To avoid this much more of rock material should be ground with all the problems mentioned in introduction.

Figure 3 presents in a log-linear scale a part of the gamma-ray spectrum of the small core-sample M2322 (Figure 1), number 2 (Table 2), counted after 7 days of decay.

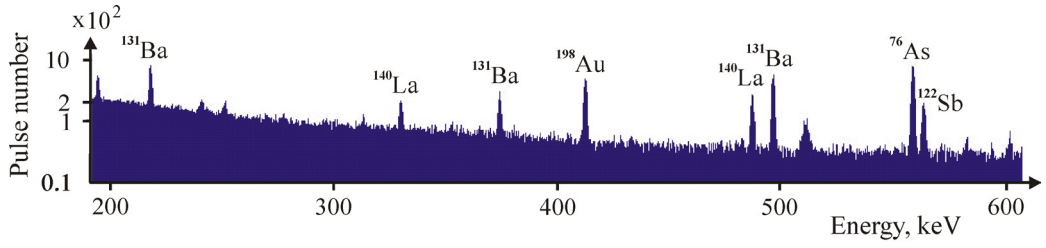

Figure 3 – A part of the gamma-ray spectrum of the small core-sample M2322(2) counted by GC2018 after 7 days of decay (in a log-linear scale)

Gamma-ray peaks of arsenic and antimony usually accompanying Au in gold deposits are noticeable, as well as some peaks of lanthanum and barium (the latter are due to the rather high Ba content about 1.5% measured in the corresponding powder sample). The volumetric sample spectrum is actually just the same as usual powder samples yield. The gist is to assess by sight sensitivity of the approach, i.e. ^{198}Au background/peak ratio, taking account of the short irradiation time (2 minutes) and a lower neutron flux in the horizontal channel. With the rather moderate Au mass fraction 0.365 μg g^{-1}, substantial potential can be noted to determine far lower Au contents in the similar way.

Figure 4(a) displaying treatment of 411.80 keV gamma-line of ^{198}Au by the "AnalGamma" software demonstrates it more visibly.

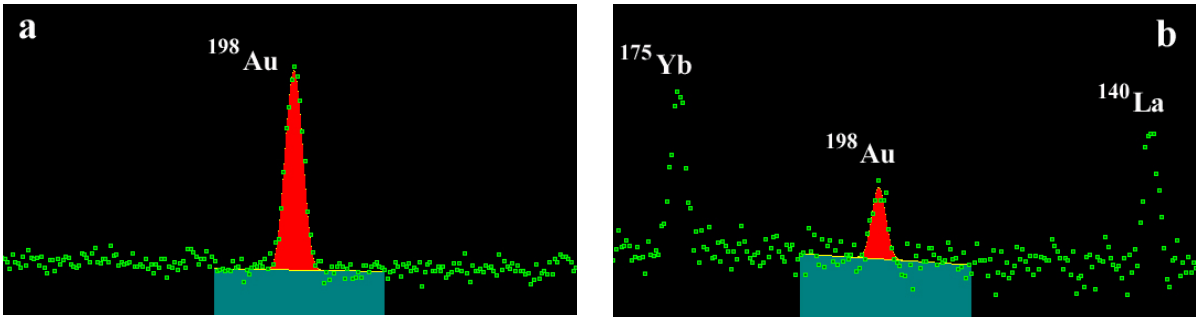

Figure 4 – Net peak area of the ^{198}Au analytical gamma-line in the "AnalGamma" treatment window: (a) – M2322(2), (b) – M2749(1)

The results of gold mass fraction determination in a range of the country rocks collected from Maikain deposit are presented in Table 3 following the same format as above. Three to five small core-samples were cut off from each lump, but only one of them is put into the table if Au content turned out lower than the limit of detection (LOD). The latter was assessed separately for every small core-sample in the same way as in [21] according to the common expression applied in the spectroscopic methods.

Table 3 – Gold content in the small core-samples and corresponding powder samples collected from the gold-polymetallic deposit Maikain, country rocks (P = 0.95)

Sample number	Description	Core-sample			Powder sample
		Mass, g	Density, g cm^{-3}	Au, μg g^{-1} (ppm)	
M1964	Gabbro dike	4.258	2.61	< 0.011	0.019 ± 0.004
M2027	Andesite-basalt rock tuff	4.161	2.61	< 0.012	0.067 ± 0.008
M2083	Sericite-quartz metasomatic rock	4.239	2.55	< 0.010	0.038 ± 0.005
M2131	Sericite-quartz metasomatic andesite	4.115 4.142 3.944 4.104	2.58 2.60 2.59 2.63	0.132 ± 0.012 0.149 ± 0.013 0.158 ± 0.014 0.166 ± 0.015	0.218 ± 0.022
M2135	Sericite-quartz metasomatic andesite	4.252 4.218 4.173 4.212	2.55 2.53 2.56 2.59	< 0.010 0.025 ± 0.005 0.018 ± 0.004 0.017 ± 0.004	0.064 ± 0.008
M2139	Sericite-quartz shale	3.730	2.34	< 0.013	0.011 ± 0.003

Table continuation

Sample number	Description	Core-sample			Powder sample
		Mass, g	Density, g cm^{-3}	Au, μg g^{-1} (ppm)	
M2394	Quartzite	4.667 4.261 4.501 4.504 4.591	2.75 2.80 2.82 2.83 2.76	0.027 ± 0.005 0.043 ± 0.007 0.017 ± 0.004 0.018 ± 0.004 0.023 ± 0.005	0.062 ± 0.008
M2401	Schistose sericite-quarts rock	3.867 4.589 4.500	2.71 2.70 2.70	0.101 ± 0.010 0.108 ± 0.011 0.108 ± 0.011	0.113 ± 0.012
M2749	Schistose sericite-quartz rock	4.059 4.261 4.518 4.247	2.66 2.62 2.66 2.61	0.035 ± 0.005 0.040 ± 0.005 0.089 ± 0.011 0.051 ± 0.006	0.072 ± 0.009
M2824	Tuff	4.374	2.63	< 0.011	0.100 ± 0.10

As Table 3 shows, gold is distributed distinctly more homogeneous in the country rocks. This probably can be explained by vast prevalence of the finely dispersed forms over the native gold, if the last is present in these rocks at all. In this connection it should be noted that Au content in the majority of the powder samples exceeds notably that of the corresponding small core-samples. The situation is like the mentioned in introduction, i.e. the part of the powder samples were seemingly contaminated with gold during grinding.

Treatment of the low-intensity gamma-line of ^{198}Au when gold mass fraction in a core-sample is close to LOD is presented in Fig. 4(b) using specimen M2749, number 1, as the example. A rather low gold content about 0.035 μg g^{-1} is surely distinguished above the background. On the whole, the LOD values of Au determination in the small core-samples after short irradiation in the horizontal channel are higher by one order of magnitude than the values usually achieved in geochemical investigations [6]. However, this scarcely can be regarded as a serious disadvantage of the approach since it is intended to analyze industrially significant gold contents which are at least two orders higher.

Conclusion

A simple variant of INAA based on the relative method of concentration standardization was used to determine Au content in the small core-samples collected from a Kazakhstan's gold-bearing deposit. The core-sample mass was restricted to approximately 10 g to provide safe operation of the automated PTS. The height and diameter of the volumetric samples (22–23 mm and ≈10 mm, respectively) are identical to the dimensions of the standard HDPE capsules filled up with the CRMs certified for Au content. So no corrections for the difference in sample geometry were necessary. Invariability of irradiation and counting geometries was ensured by the construction of the irradiation terminal and by the special Plexiglas attachment mounted on the detector cap. Due to the substantial difference in the densities of the CRMs and the small core-samples, corrections for neutron self-shielding and self-absorption of ^{198}Au analytical gamma-line were applied. The first one never exceeded 2% in the solid samples regardless of Au content, the latter reached 11% (both relatively to that for the CRMs). Influence of the neutron flux gradient during irradiation was eliminated owing to the centrally symmetric counting geometry.

INAA of small core-samples doesn't need any unique equipment, only the automated PTS, research reactors are usually equipped with. The tried approach can't solve all the problems connected with gold determination in highly heterogeneous ores. However, it can promote substantially to assess gold resources provided the small core-samples are collected in-situ and the methods of geostatistics are used to interpret the results.

Acknowledgments

The work was supported by the grants BR23891691 from the Ministry of Energy of the Republic of Kazakhstan and BR10264324 from the Committee of Geology under the Ministry of Ecology, Geology and Mineral Resources of the Republic of Kazakhstan.

References

1. Gas'kov I.V. (2017) Major impurity elements in native gold and their association with gold mineralization settings in deposits of Asian folded areas. *Russ Geol Geophys*, vol. 58(9), pp. 1080-1092. http://doi.org/10.1016/j.rgg.2017.08.004.

2. Matvienko V.N., Kalashnikov Y.D., Goncharov A.A. (2014) Natural clusters as the source of ore material formation in noble metals deposits: case study of gold fields in the Republic of Kazakhstan, Russia, Uzbekistan, and Kyrgyzstan. *Life Sci J*, vol. 11(1), pp. 269-281.

3. Dominy S.C., Platten I.M. (2007) Gold particle clustering: a new consideration in sampling applications. *Appl Earth Sci*, vol. 116(3), pp. 130-142. https://doi.org/10.1179/174327507X207474.

4. Pitcairn I.K. (2011) Background concentrations of gold in different rock types. *Appl Earth Sci*, vol. 120(1), pp. 31-38. https://doi.org/10.1179/1743275811Y.0000000021.

5. Balaram V. (2008) Analytical methods for gold and other precious metals in exploration studies. *J Appl Geochem*, vol. 10(2A), pp. 545-562.

6. Silachyov I.Yu., Glagolev V.A. (2022) Comparator neutron activation analysis of the solid volumetric rock samples for gold content. *IJBCh*, vol. 15(1), pp. 90-101. https://doi.org/10.26577/ijbch.2022.v15.i1.010.

7. Balaram V. (2008) Recent advances in the determination of PGE in exploration studies – A review. *J Geol Soc India*, vol. 72, pp. 661-677.

8. Balaram V., Subramanyam K.S.V. (2022) Sample preparation for geochemical analysis: Strategies and significance. *Adv Sample Prep*. https://doi.org/10.1016/j.sampre.2022.100010.

9. Alsufyani S.J., Liegey L.R., Starovoitova V.N. (2014) Gold bearing ore assays using ^{197}Au (γ, n) ^{196}Au photonuclear reaction. *J Radioanal Nucl Chem*, vol. 302(1), pp. 623-629. https://doi.org/10.1007/s10967-014-3239-2.

10. Lee M., Norman E.B., Akindele O.A., et al. (2022) Fast neutron activation of ubiquitous materials. *Appl Radiat Isot*, vol. 181, p. 110098. https://doi.org/10.1016/j.apradiso.2022.110098.

11. Marchese N., Cannuli A., Caccamo M.T., et al. (2017) New generation non-stationary portable neutron generators for biophysical applications of neutron activation analysis. *Biochim Biophys Acta*, vol. 1861(1), pp. 3661-3670. http://dx.doi.org/10.1016/j.bbagen.2016.05.023.

12. Nat A., Ene A., Lupu R. (2004) Rapid determination of gold in Romanian auriferous alluvial sands, concentrates and rocks by 14 MeV NAA. *J Radioanal Nucl Chem*, vol. 261(1), pp. 179-188. https://doi.org/10.1023/B:JRNC.0000030954.29323.39.

13. Rodríguez N., Yoho M., Landsberger S. (2016) Determination of Ag, Au, Cu and Zn in ore samples from two Mexican mines by various thermal and epithermal NAA techniques. *J Radioanal Nucl Chem*, vol. 307(2), pp. 955-961. https://doi.org/10.1007/s10967-015-4277-0.

14. Nyarku M., Nyarko B.J.B., Serfor-Armah Y., et al. (2010) Investigating concentration distributions of arsenic, gold and antimony in grain-size fractions of gold ore using instrumental neutron activation analysis. *Appl Radiat Isot*, vol. 68(2), pp. 378-383. https://doi.org/10.1016/j.apradiso.2009.10.010.

15. Bode P., Romanò S., Romolo, F.S. (2018) Large sample neutron activation analysis avoids representative sub-sampling and sample preparation difficulties: an added value for forensic analysis. *Forensic Chem*, vol. 7, pp. 81-87. https://doi.org/10.1016/j.forc.2017.10.002.

16. Menezes M.Â., Jaćimović R. (2014) Implementation of a methodology to analyse cylindrical 5-g sample by neutron activation technique, k_0 method, at CDTN/CNEN, Belo Horizonte, Brazil. *J Radioanal Nucl Chem*, vol. 300(2), pp. 523-531. https://doi.org/10.1007/s10967-014-3074-5.

17. Farina Arboccò F., Vermaercke P., Sneyers L., et al. (2012) Experimental validation of some thermal neutron self-shielding calculation methods for cylindrical samples in INAA. *J Radioanal Nucl Chem*, vol. 291(2), pp. 529-534. https://doi.org/10.1007/s10967-011-1211-y.

18. Sudarshan K., Nair A., Goswami A. (2003) A proposed k_0 based methodology for neutron activation analysis of samples of non-standard geometry. *J Radioanal Nucl Chem*, vol. 256(1), pp. 93-98. https://doi.org/10.1023/A:1023356227170.

19. Kokkuzova M., Bekenova G., Dyussembayeva K., et al. (2017) Gold-barite-polymetallic VMS deposit of Maikain, NE Kazakhstan. *Appl Earth Sci*, vol. 126(2), pp. 71-72. https://doi.org/10.1080/03717453.2017.1306266.

20. Kokkuzova M., Bekenova G., Dyussembayeva K. (2016) Gold-telluride association in the ores of gold-polymetallic deposits of Rudny Altai and Central Kazakhstan. *16th International Multidisciplinary Scientific GeoConference SGEM 2016*, Sofia, Bulgaria, vol. 2, pp. 1081-1088.

21. Silachyov I.Yu. (2021) Determination of indium in its ore resources by comparator neutron activation analysis. *IJBCh*, 14(2), 106-116. https://doi.org/10.26577/ijbch.2021.v14.i2.015.

22. Ismail S.S. (2010) A new automated sample transfer system for instrumental neutron activation analysis. *J Autom Methods Manage Chem*, vol. 2010(1), 8 pp. https://doi.org/10.1155/2010/389374.

23. Evaluation of measurement data – Guide to the expression of uncertainty in measurement. JCGM, 2008, 120 p.

24. Silachyov I. (2023) Zircon concentrate analysis for sixteen rare earth elements by the complex of nuclear analytical methods. *J Radioanal Nucl Chem*. Published online. https://doi.org/10.1007/s10967-023-08844-1.

25. Silachyov I.Yu. (2020) Instrumental neutron activation analysis of rhenium in uranium raw material. *IJBCh*, vol. 13(1), pp. 161-169. https://doi.org/10.26577/ijbch.2020.v13.i1.17.

26. Chilian C., St-Pierre J., Kennedy G. (2008) Complete thermal and epithermal neutron self-shielding corrections for NAA using a spreadsheet. *J Radioanal Nucl Chem*, vol. 278(3), pp. 745-749. https://doi.org/10.1007/s10967-008-1604-8.

27. Rudnick R.L., Gao S. (2014) Composition of the continental crust. In: Holland H.D., Turekian K.K. (Ed.) Treatise on Geochemistry, 2nd edition, vol. 4. Elsevier, pp. 1-51. https://doi.org/10.1016/B978-0-08-095975-7.00301-6.

28. Haynes W.M. (Ed.) (2016) Abundance of elements in the earth's crust and in the sea. CRC handbook of chemistry and physics, 97th edition. Boca Raton, Florida: CRC press, pp. 14-17. ISBN: 9781498754286.

29. Hubbell J.H., Seltzer S.M. (accessed May 15, 2023) X-ray mass attenuation coefficients. NIST standard reference database 126. https://www.nist.gov/pml/x-ray-mass-attenuation-coefficients.

30. OST 41-08-212-04 (2004) Standart otrasli. Upravlenie kachestvom analiticheskih rabot. Normy pogreshnosti pri opredelenii himicheskogo sostava mineralnogo syr'ya i klassifikatsiya metodik laboratornogo analiza po tochnosti rezultatov (Idustrial standard. Quality management of analytical work. Error guidelines for chemical analysis of mineral resources and precision classification of laboratory analytical techniques). Moscow, VIMS, 23 p. (in Russian).

31. Nuclear data sub-committee. K0-neutron activation analysis link page (accessed May 15, 2023). http://www.kayzero.com/k0naa/k0naaorg/Links.html.

Information about authors:

Igor Yurievich Silachyov – candidate of engineering sciences, Institute of Nuclear Physics (Almaty, Kazakhstan, e-mail: silachyov@inp.kz

Glagolev Vladimir Andreyevich – senior research fellow, The Institute of Geological Sciences n.-a. K. I. Satpayev (Almaty, Kazakhstan; vaglag@mail.ru)

Kokkuzova Manshuk – Master of Technical Sciences, The Institute of Geological Sciences n.-a. K. I. Satpayev (Almaty, Kazakhstan; m.kokkuzova@satbayev.university)